Modeling the Effect of Bubble Plumes on High Frequency Acoustic Propagation in Shallow Water

C. Allan Boyles
Johns Hopkins University
Applied Physics Laboratory
Laurel, MD, 20723
Email: Allan.Boyles@jhuapl.edu

Allan P. Rosenberg
Johns Hopkins University
Applied Physics Laboratory
Laurel, MD, 20723
Email:Allan.Rosenberg@jhuapl.edu

Qinqing Zhang
Johns Hopkins University
Applied Physics Laboratory
Laurel, MD, 20723
Email: Qinqing.Zhang@jhuapl.edu

Abstract—**In this paper we model the effect of bubbles on high frequency acoustic propagation in shallow water under strong winds. Underwater bubble clouds provide locally significant modifications of the sound speed field. The modified sound speed field contributes to a major transmission loss to sound propagation and scattering of the signals. We adopt the bubble field model developed by Norton, et al., generate range dependent discrete bubble plumes and compute the sound speed profile of each bubble plume. We expand our previous work on modeling the effect of rough sea surface and bubble plumes, to include both β- and γ-plumes in the model. We particularly compare cases where the random distribution of β- and γ-plumes are generated differently. With a bubble perturbed sound speed field, we model the communication channel using a rough surface parabolic equation model to generate a complex pressure field at a selected set of ranges and depths. These pressure fields form the basic frequency response of the channel. Our results show that under strong winds, bubbles contribute to large transmission loss and cannot be neglected. The dominant contribution to attenuation is due to β plumes rather than γ plumes. However γ plumes cannot be ignored because their existence affects the spacing between β plumes. And the spacing between β plumes is a significant factor, which results in less attenuation compared to closely spaced β plumes.**

I. INTRODUCTION

Underwater acoustic communication is extremely difficult due to diverse and dynamic environmental factors. Especially in shallow water, sound waves propagate along a narrow water waveguide and bounce between surface and bottom frequently. Even under calm conditions, many locations exhibit strong multipath propagation, which causes signal variation and large spread in both time and frequency. When wind picks up or swell generated elsewhere moves into the sea, the surface roughens and changes over time. Furthermore wave breaks, ultimately producing underwater bubble clouds. These bubbles eventually dissipate but in the meantime provide locally significant modifications of the sound speed field. Internal tides and internal waves also affect the propagation. Many of these phenomena will affect a high frequency, wide-band acoustic signal more than a low frequency and narrow-band one. Understanding and characterizing this variability is essential in designing adaptive techniques for communication waveforms and signal processing to ensure efficient and reliable communication.

In this paper, we address the effect of bubble plumes on high frequency acoustic propagation, which are dominant factors affecting the performance of acoustic communications in shallow water. G. Norton, J. Novarini, and R. Keiffer have published a seminal series of papers [1], [2] which model acoustic propagation in a shallow water waveguide with a randomly rough sea surface, and bubble plumes. In [1] they developed a bubble plume model based on existing bubble measurement data. In [2] they investigated the relative role of sea-surface roughness and bubble plumes in shallow water propagation for the frequency range 2 - 4 kilohertz (kHz). Even though Norton and Novarini only investigated the effect on propagation due to bubbles in the 2 - 4 kHz range, the bubble model is valid up to several hundred kHz as can be seen in [1]. Norton and Novarini have shown in [2] that a bubble field must correctly be modeled by discrete plumes, because the representation of a bubble field by a range independent layer shows contradictory results on the influence of bubbles. They further show that scattering from the plumes is the major loss mechanism, and not refraction. We adopt their bubble plume model to generate range dependent discrete bubble plumes and the perturbed sound speed field.

We expand our previous work on modeling the effect of rough sea surface and bubble plumes [3], to include both β- and γ-plumes in the model. We develop the model to compute the bubble spectra and generate the bubble modified sound speed fields in shallow water under high winds. We particular compare cases where the random distribution of β- and γ-plumes are generated differently. We then use our developed rough surface parabolic equation model [4] to produce a complex pressure field at selected range and depth points. These pressure fields are the basic data for channel characterization.

The paper is organized as follows. Section II describes the β- and γ-plumes model based on the methods developed by Norton, Novarini, et al. Section III provides the numerical results of bubble spectra and sound speed fields using the modeling approach described in section II. Section IV presents

978-0-933957-40-4 ©2013 MTS

This is a DRAFT. As such it may not be cited in other works. The citable Proceedings of the Conference will be published in IEEE Xplore shortly after the conclusion of the conference.

the effect of bubbles and their random distribution on channel propagation. Finally section V concludes the paper.

II. BUBBLE PLUME MODEL

A. Introduction

The microbubble layer underlying the ocean surface can be pictured as patchy clouds on a persistent background. Based on previous measurements and his own observations, Monahan [5], [6] assumed the existence of three types of plumes which he called α-, β-, and γ-plumes, and associated the α- and β-plumes with stages A and B of whitecaps, respectively. Stage A is associated with the crest of the spilling breaker, and Stage B is associated with the foam patch.

The α-plume is the subsurface expression of the stage A whitecap. They are small in size and last less than a second so they can be ignored. The α-plume quickly decays into the β-plume. Accordingly, the stage A whitecap evolves into a foam patch – the stage B whitecap. The β-plumes are attached to the foam patch. They have a lifetime of about 4 seconds. The β-plumes then evolve into the γ-plumes and eventually detach from the originating whitecap. Their lifetimes are 10-100 times longer than the β-plumes. Finally, the γ-plumes decay into the weak stratified background layer.

G. Norton and J. Novarini arrived at the following conclusions: (1) the representation of a bubble field by a range independent layer shows contradictory results on the influence of bubbles, so that a bubble field must correctly be modeled by discrete plumes; (2) the main mechanism responsible for the excess loss at high wind speeds in shallow-water waveguides seems to be the patchy nature of the subsurface bubble field; (3) the β-plumes provide the dominant mechanism that attenuates the field; (4) at least for frequencies between 2 - 4 kHz the attenuation inside the β-plumes has essentially no effect on the transmission loss; and (5) the spacing of the β-plumes has a big impact on the results.

Based on these conclusions, in our previous work [3], we focused on the β-plumes in our calculations only, and neglected the attenuation within the plumes. In this paper, we include both β- and γ-plumes in the model and compare the mixed plumes model with our previous results.

B. The bubble plume model

The bubble population of each type of the plume has the form

$$n(a,z,u) = N_0 G(a) Z(z) U(u), \qquad (1)$$

where $n(a,z,u)$ is the number of bubbles per m^3 per μm, of radius $a(\mu m)$, at depth $z(m)$ for a wind speed $u(m/s)$ measured at $10m$ height above the sea surface. $G(a)$ is the spectral function, $Z(z)$ is the depth dependent function and $U(u)$ is the velocity function. N_0 is the bubble density at the surface. The constant N_0 is chosen so that it leads to values for the bubble density within the range specified by Monahan for the concentration and the void fraction of the β-plume.

Each type of plume has different values for G and Z. However, for all types of plumes U is taken to be

$$U(u) = \left(\frac{u}{13}\right)^3 \qquad (2)$$

B.1 β plumes

For β-plumes Eq.(1) becomes

$$n_\beta(a,z,u) = N_{0\beta} G_\beta(a) Z_\beta(z) U(u) \qquad (3)$$

The spectral function for the β-plumes is given by

$$G_\beta(a) = \begin{cases} 0, & a < a_{min} \\ (a/a_1)^3, & a_{min} \le a < a_1 \\ 1, & a_1 < a \le a_2 \\ (a_2/a)^4, & a_2 < a \le a_3 \\ (a_2/a_3)^4 (a_3/a)^{2.6}, & a > a_3 \end{cases} \qquad (4)$$

where

$a_{min} = 10\ \mu m$

$a_1 = 15\ \mu m$

$a_2 = 20\ \mu m$

$a_3 = 60\ \mu m$

The depth dependent function for the β-plumes is given by

$$Z_\beta(z) = \begin{cases} 1, z \le z_{\beta max} \\ 0. \ z > z_{\beta max} \end{cases} \qquad (5)$$

where $z_{\beta max} = 1.23 \times 10^{-2}\, u^2$.

The bubble density at the surface is

$$N_{0\beta} = 2.0 \times 10^7 \ (m^{-3} \mu m^{-1}) \qquad (6)$$

The β-plume has a horizontal cross-section whose area $A(z)(m^2)$ decays exponentially with depth according to

$$A(z) = A_0 \exp(-z/d) \qquad (7)$$

where $d = z_{\beta max}/5.99$. For the β-plume, the area of the stage B foam patch determines the size of the plumes at the surface. The area of the foam patch can be estimated from

$$A_0 = 17.0 + 0.0307(u - 5)^2 \qquad (8)$$

In this one-dimensional representation of the plume, we use the square root of the area, denoted by $L_\beta(z)$, as the equivalent horizontal length of the plume, then

$$L_\beta(z) = L_{0\beta}\exp\left(-\frac{z}{2d_\beta}\right)$$

$$L_{0\beta} = L_\beta(z=0) = (17.0 + 0.0307(u-5)^2)^{\frac{1}{2}} \quad (9)$$

$$d_\beta = z_{\beta max}/5.99$$

where $L_0=(A_0)^{1/2}$.

To complete the description we need to specify their distribution in range. Since the β-plumes are attached to stage B whitecaps, the spacing S_β in meters, between β-plumes is set equal to the spacing between foam patches, which is given by

$$S_\beta = (237)\, u^{-1.07} \quad (10)$$

B.2 γ plumes

For γ-plumes Eq.(1) becomes

$$n_\gamma(a,z,u) = N_{0\gamma}G_\gamma(a)Z_\gamma(z)U(u), \quad (11)$$

The spectral function for the γ-plumes is given by

$$G_\gamma(a) = \begin{cases} 0, & a < a_{min} \\ (a/a_1)^3, & a_{min} \le a < a_1 \\ 1, & a_1 < a \le a_2 \\ (a_2/a)^4, & a_2 < a \le a_3 \\ (a_2/a_3)^4(a_3/a)^{p(z)}, & a > a_3 \end{cases} \quad (12)$$

where

$$a_{min} = 10\ \mu m$$

$$a_1 = 15\ \mu m$$

$$a_2 = 20\ \mu m$$

$$a_3 = 60\ \mu m.$$

$$P(z)=4.37+(z/2.55)^2$$

The bubble density at the surface is

$$N_{0\gamma} = 6.0\times 10^5\ (m^{-3}\mu m^{-1}) \quad (13)$$

The depth dependent function for the γ-plumes is given by

$$Z_\gamma(z) = e^{-z/d_\gamma} \quad (14)$$

Hall [7] and Wu [8-9] obtain a simpler expression base on Thorp's results [10]. This result was used in our computing model.

$$d_\gamma = \begin{cases} 0.4, & u \le 7.5\ m/s \\ 0.4 + 0.115(u-7.5), & u > 7.5\ m/s \end{cases} \quad (15)$$

Monahan describes the γ-plume as having a cross section that decays exponentially with depth. From Monahan's parameterization, the area at the surface can be estimated to be approximately nine times that of the β-plumes. Hence its equivalent length at the surface is three times that of the β-plumes. Therefore

$$L_\gamma(z) = 3L_{0\beta}\exp\left(-{}^{z}/_{2d_\gamma}\right) \quad (16)$$

As for the spatial distribution of the γ plumes, it can be assumed that close to the surface they are contiguous to each other.

C. Background layer

Concerning the persistent background layer, the bubble density is adopted that has the same spectral form as that used for the γ-plumes but with a much lower density and penetration. The spectral density is then given by

$$n_{bl}(a,z,u) = N_{0bl}G_{bl}(a)Z_{bl}(z)U(u) \quad (17)$$

The spectral function is the same as for the γ-plumes shown in Eq. (12).

The bubble density at the surface is

$$N_{0bl} = 2.0\times 10^4\ (m^{-3}\mu m^{-1}) \quad (18)$$

The depth function is assumed to have a form suggested by Hall [7],

$$Z_{bl}(z) = e^{-z/d_{bl}},$$

$$d_\gamma = \begin{cases} 0.4, & u \le 7.5\ m/s \\ 0.4 + 0.115(u-7.5), & u > 7.5\ m/s \end{cases} \quad (19)$$

D. Speed of sound in a bubbly mixture

To calculate the effective speed of sound in a bubbly medium, an approach is used based on the compressibility of the mixture which renders an effective sound speed for linear pressure waves in a bubbly medium [11]. The presence of oscillating bubbles causes the medium to be dispersive.

Let C_{eff} be the complex effective sound speed (m/s) in the bubbly mixture, C_0 the background sound speed (m/s), C_p the phase speed (m/s), α the attenuation (dB/m), and f_r the resonant bubble frequency (Hz). Then

$$\frac{1}{C_{eff}^2} = \frac{1}{C_0^2} + \frac{1}{\pi f^2}\int_{a_{min}}^{a_{max}}\left\{\frac{a\cdot n(a)da}{[\frac{f_r^2}{f^2}-1+i\delta]}\right\} \quad (20)$$

where

$$f_r = (1+0.1z)^{\frac{1}{2}}\left(\frac{3.25\times 10^6}{a}\right),$$

and $$a_{max} = 1000\exp\left(-\frac{z}{4.1}\right).$$

The phase velocity and attenuation are then given by

$$C_p = real(C_{eff}), \quad (21)$$

and

$$\alpha = - \frac{20\omega}{ln10} im(\frac{1}{C_{eff}}) \quad (22)$$

E. Statistical fluctuation of bubble parameters

To simulate ocean experiments the bubble concentration, N_0, the plume depth, z_{max}, the size of the foam patch, *L*, and the spacing between plumes, *S*, is randomized.

There is not enough information in the literature to quantify all the statistical deviations necessary to randomize the model. Norton, Novarini, and Keiffer assume a 20% variation for N_0 and *S.* A 30% variation is allowed for plume depth, z_{max}, and the equivalent length, *L*.

III. NUMERICAL RESULTS OF BUBBLE PLUMES

We compute the bubble spectra and the effective sound speed using the analysis in Section II.

Figure 1a shows the bubble spectrum for a β-plume evaluated at z = 0.2 m depth and a wind speed of 12 m/s using Eq. (1) – (10). Figure 1b shows the bubble spectrum for a γ-plume evaluated at z = 0.2m and a wind speed of 12 m/s using Eq. (11) – (16).

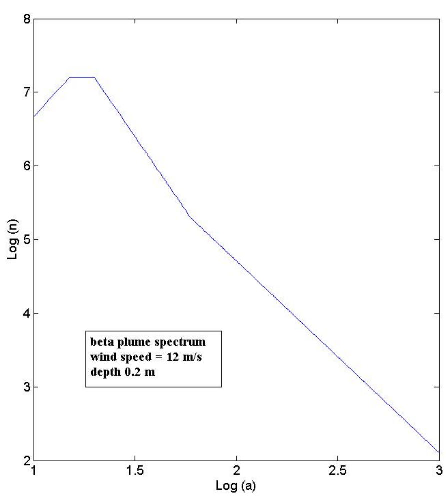

Figure 1a. Bubble spectrum for a β-plume evaluated at z=0.2m and a wind speed of 12 m/s.

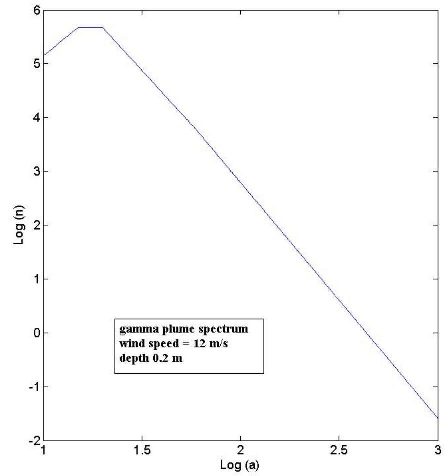

Figure 1b. Bubble spectrum for a γ-plume evaluated at z=0.2m and a wind speed of 12 m/s.

Figure 2 shows the sound speed profile versus depth along the axis of a β-plume at 12.5 kHz and a wind speed of 12 m/s. Figure 3 shows the sound speed profile versus depth along the axis of a γ-plume at 12.5 kHz and a wind speed of 12 m/s.

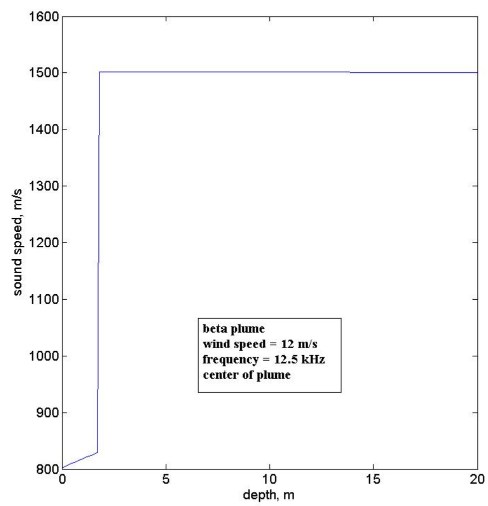

Figure 2. Sound speed profile versus depth along axis of a β-plume at 12.5 kHz and a wind speed of 12 m/s.

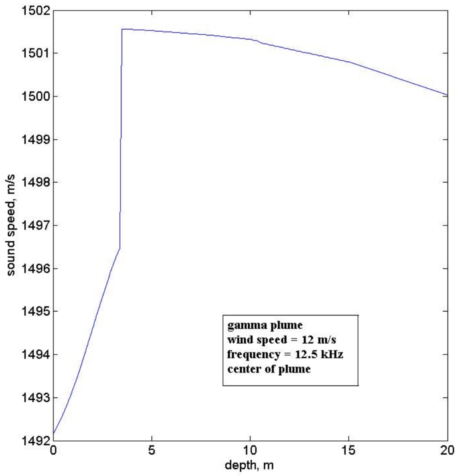

Figure 3. Sound speed profile versus depth along axis of a γ-plume at 12.5 kHz and a wind speed of 12 m/s.

Figure 4 shows a single β-plume at a wind speed of 12 m/s and frequency of 12.5 kHz. Figure 4 shows a single γ-plume at a wind speed of 12 m/s and frequency of 12.5 kHz.

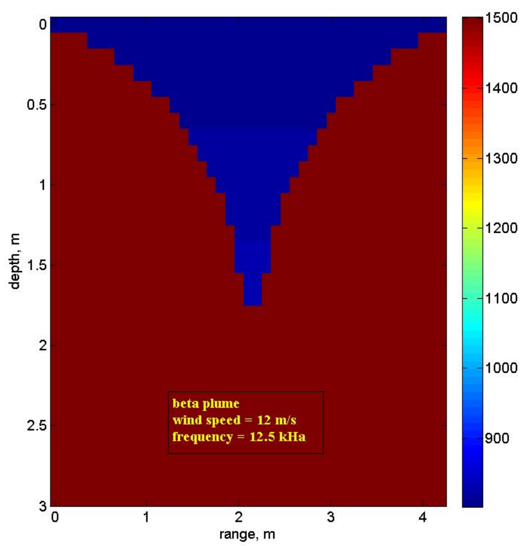

Figure 4. One β-plume at 12.5 kHz and a wind speed of 12 m/s.

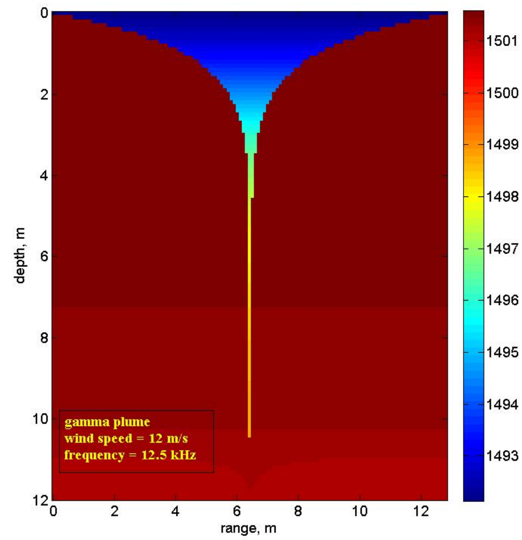

Figure 5. One γ-plume at 12.5 kHz and a wind speed of 12 m/s.

IV. EFFECT OF BUBBLE PLUMES ON PROPAGATION

In this section we examine the effect of a bubble perturbed sound speed field on the propagation of sound waves. In our previous work [3], we observed that there was not much difference between the transmission loss for the cases of a flat surface and a rough surface when bubble plumes were present. Consequently, for high wind speeds the dominant attenuation mechanism is the scattering from bubble plumes rather than scattering from a rough sea surface. Based on this observation, we use a flat surface in our parabolic equation (PE) modeling for the propagation computation [4]. Unless otherwise indicated all the plots in this section are for a point source at a depth of 11.1 meters with a center frequency of 12.5 kHz. The bubble perturbed sound speed fields that we use are also for that center frequency. An ensemble average of the intensity was taken over the realizations.

Figure 6 shows a picture of whitecaps approximately 160m x 160m of the sea surface taken from an altitude of 400m for a mean wind speed of 13.6 m/s [12]. Since our propagation model is 2-dimensional, we can only calculate propagation along the path defined by a bubble plume, which we call a "*track*". Therefore we looked at various tracks. We see that there are tracks where the spacing of the foam closely matches Norton's spacing S_β, and other tracks where there are large gaps between the foam patches (β plumes). Because of these random tracks of plumes and associated spacing, we examine the following three cases. (1) A random distribution along a track of β-plumes and γ-plumes, where the β-plumes are widely separated and the γ-plumes fill in the spaces between the β-plumes. (2) The same track distribution of β-plumes and γ-plumes as in case (1), except the bubble distribution in the γ-plumes was replaced with the background layer. (3) A random distribution of β-plumes only which are separated by S_β. This is basically the case we analyzed in our previous work [3]. Comparison between case (1) and (2) would show whether γ-plumes contribute significantly to the propagation loss. Comparison between case (1) and (3) would show how critical the spacing is for the β-plumes and would further verify the observation noted by Norton, et al.

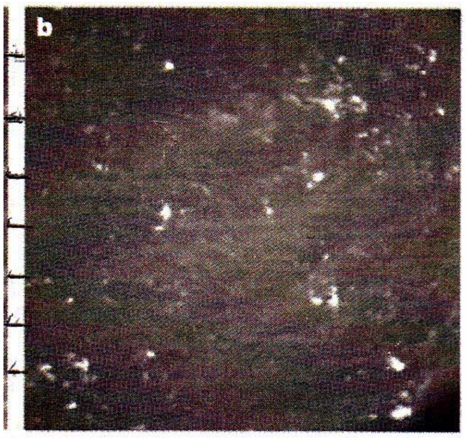

Figure 6. Aerial image of whitecaps approximately 160m x 160m of the sea surface taken from an altitude of 400m for a mean wind speed of 13.6 m/s

Figure 7 shows one possible random track of β plumes and γ plumes as of case (1). The β plumes actually have sound speeds down to about 800 m/s, but if a color code was used which went from 800m/s to 1500m/s, the γ plumes would not be visible. Figure 8 shows one possible random track of β plumes as of case (3). The β plumes are closely separated by S_β. Note that the depth scales are different on Figures 7 and 8.

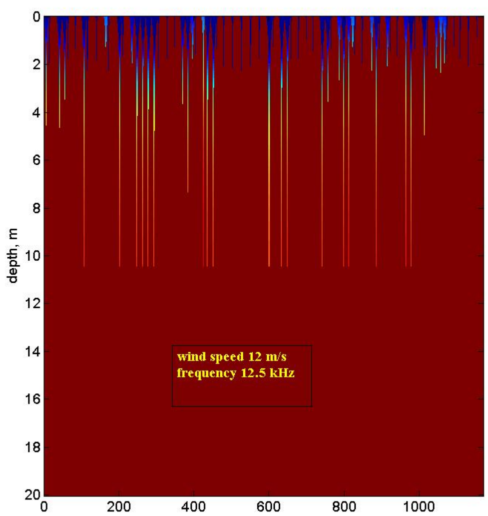

Figure 7. A random track of β-plumes and γ-plumes, case (1)

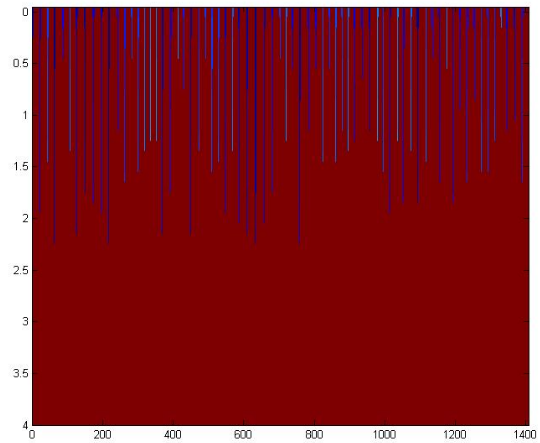

Figure 8. A random track of β-plumes, case (3)

Next we compare the transmission loss of sound propagation in the three cases. Figure 9 shows the field plot generated using a range independent reference sound speed profile under a flat surface. This is the case without any bubble. Figure 10 shows the field plot of a random distribution along a track of β-plumes and γ-plumes, where the β-plumes are widely separated and the γ-plumes fill in the spaces between the β-plumes. This is case (1). Figure 11 shows field plot of the same track distribution of β plumes and γ plumes as in case (1), except the bubble distribution in the γ plumes was replaced by the bubble distribution of the background layer. This is case (2). Figure 12 shows the field plot of a random distribution along a track of β-plumes only which are separated by S_β. This is case (3).

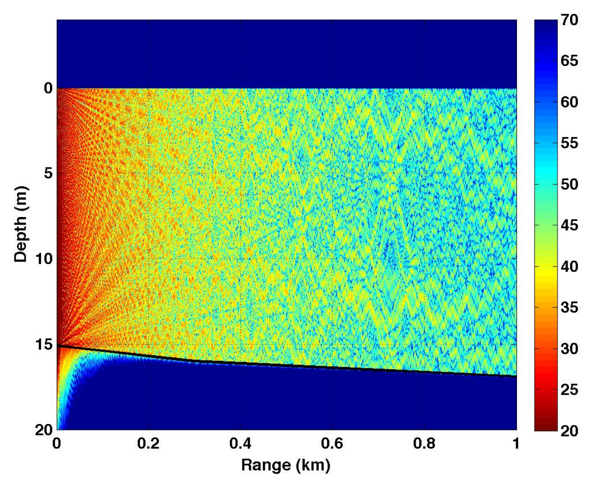

Figure 9. Field plot of no bubbles

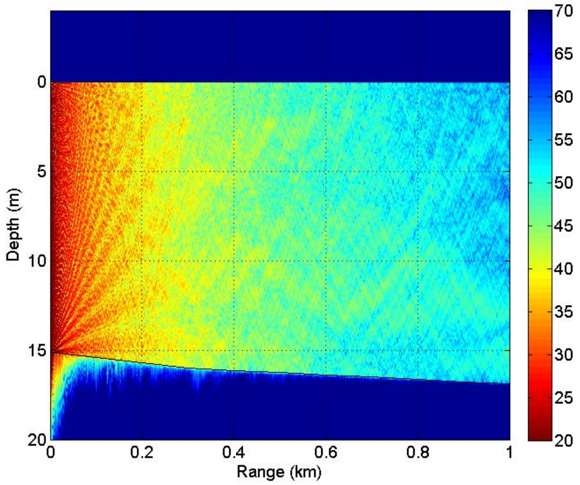

Figure 10. Field plot of a random distribution along a track of β-plumes and γ-plumes, case (1).

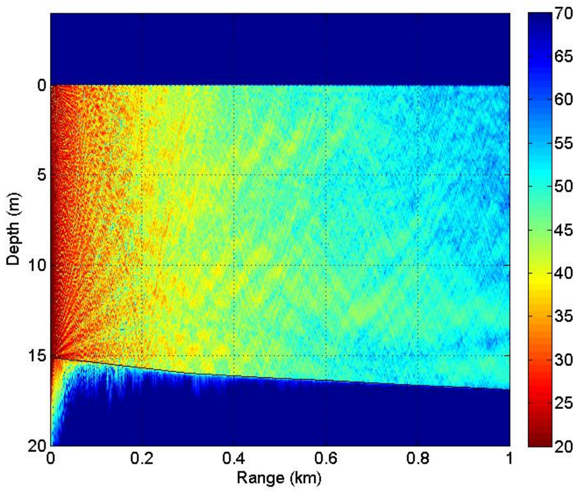

Figure 11. Field plot of a random distribution along a track of β-plumes and the background layer, case (2).

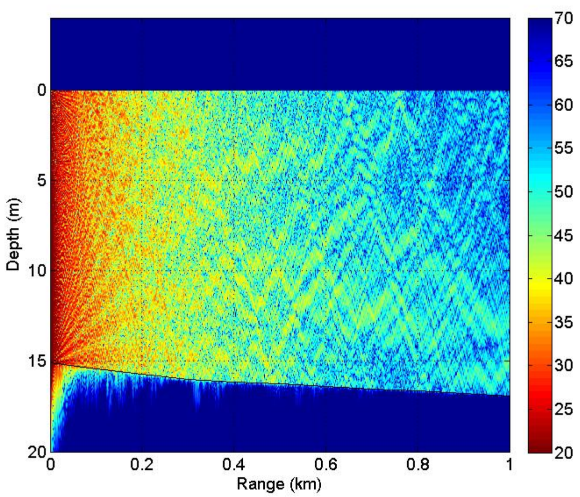

Figure 12. Field plot of a random distribution of β-plumes only which are separated by S_β, case (3).

Comparing the three cases with the no bubble case in Figure 9, we see that the presence of bubbles causes considerable loss. This is further evident as shown in Figure 13 and Figure 14. Figure 13 compares the transmission loss difference among no bubble case, case (1) and case (2) at z = 10m depth. Figure 14 compares the transmission loss difference among no bubble case, case (1) and case (3) at z = 10m depth.

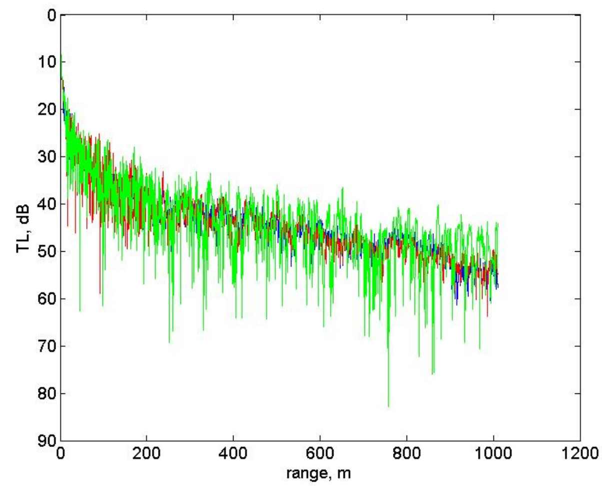

Figure 13. Comparison of transmission loss for no bubbles (green), case (1) (blue) and case (2) (red) at z=10m depth.

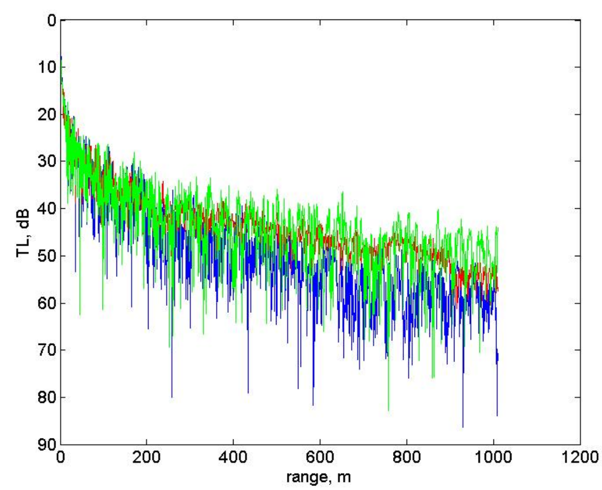

Figure 14. Comparison of transmission loss for no bubbles (green), case (1) (red) and case (3) (blue) at z=10m depth.

We observe that there is negligible difference between transmission loss for case (1) and case (2) as shown in Figure 13. In other words, the propagation with and without γ plumes is not much different. As shown in Figure 14, we see that there is significant difference between transmission loss for case 1 and case 3. This indicates that the spacing between β plumes is a significant factor. It also shows that along tracks where β plumes are spaced by S_β (case (3)), there is considerable attenuation from the case of no bubbles.

V. CONCLUSIONS

In this paper, we adopt the bubble plume model developed by Norton et al, and generate the bubble modified sound speed fields in shallow water under high winds. We conclude that at high wind speed bubbles cannot be neglected. The bubble plumes create a much reduced sound speed field near the surface and affect the sound propagation dramatically. Following Norton and Novarini, we recommend that a bubble field must be modeled by discrete plumes rather than a range independent bubble layer. In a previous paper [3] we examined the effect of the discrete bubble plumes on acoustic signal propagation under both a flat surface and rough surface. We observed that both bubbles and rough surface contribute to large transmission loss. The transmission loss caused by bubbles is much more than the loss caused by rough surface. Consequently, for high wind speeds the dominant attenuation mechanism is the scattering from bubble plumes rather than scattering from a rough sea surface. Therefore in this paper we ignore the rough sea surface and assume a flat surface. For this study we include γ plumes as well as β plumes. We conclude that the dominant contribution to attenuation is due to β plumes since they have a higher bubble density. Norton et al, also found this to be true for their case. However, γ plumes cannot be ignored because their presence affects the spacing between β plumes. The spacing between β plumes is a significant factor affecting the attenuation of sound propagation. In our previous paper [3] we used an observed spacing, S_β between β plumes. As seen in Figure 6 β plumes along some tracks, i.e., the paths defined by the bubble plumes, can be spaced much greater than S_β and this results in less attenuation. We know that under windy conditions there exist many γ plumes between β plumes. So while only β plumes need to be considered, tracks with realizations of spacing greater than S_β need to be considered, but not with a spacing less than S_β.

More detailed channel characterizations under rough surface with bubbles are currently under investigation and results will be reported in the near future.

REFERENCES

[1] J. C. Novarini, R. S. Keiffer, and G. V. Norton, “A model for variations in the range and depth dependence of the sound speed and attenuation induced by bubble clouds under wind-driven conditions,” *IEEE J. Ocean Engineering,* Vol. 23, pp 423-438, October 1998.

[2] Guy V. Norton and J. C. Novarini, “On the relative role of sea-surface roughness and bubble plumes in shallow-water propagation in the low-kilohertz region,” *J. Acoust. Soc. Am*., Vol. 110, pp 2946-2955, December 2001.

[3] C. A. Boyles, A. P. Rosenberg, and Q. Zhang, “Underwater Acoustic Communication Channel Characterization in the Presence of Bubbles and Rough Sea Surfaces,” *IEEE/MTS Oceans 2011 Conference*, Santander, Spain, June 2011.

[4] A. P. Rosenberg, D. Chizhik, Q. Zhang, “High Frequency Rough Surface Parabolic Equation Modeling for Underwater Acoustic Communications,” *Proceedings of IEEE Milcom2009*, Boston, MA, USA, October 2009.

[5] E. C. Monahan, *in Proc. 7th Conf. on Ocean-Atmosphere Interaction, Anaheim, CA , Am. Meter. Soc*., 1988, pp 178-181.

[6] E. C. Monahan and M. Lu, “Acoustically relevant bubble assemblages and their dependence on meteorological parameters.” *IEEE J. Ocean Engineering*, Vol. 15**,** pp 340-349, 1990.

[7] M. V. Hall, “A comprehensive model of wind generated bubbles in the ocean and the predictions of the effects on sound propagation at frequencies up to 40kHz,” *J. Acoust. Soc. Am*., **86** (1989), 1103-1116.

[8] J. Wu, “Bubbles in the near surface ocean: A general description,” *J. Geophy. Res,*. Vol 93, No. C1, 587-590, January 15, 1988.

[9] J. Wu, “Individual characteristics of whitecap and volumetric description of bobbles,” *IEEE J. Oceanic Eng*., Vol. 17, No. 1, 150-158, January 1992.

[10] S. A. Thorpe,”On the clouds of bubbles formed by breaking waves in deep water and their role in the air-sea transfer,” Philos. Trans. R. Soc. London Ser. A, vol. 304. Pp. 155-210, 1982.

[11] C. S. Clay and H. Medwin, *Acoustical Oceanography*, *John Wiley and Sons,* 1977, Appendix A6.

[12] W. K. Melville and P. Matusov, “Distribution of breaking waves at the ocean surface,” *Nature,* Vol 417, May 2002.